Journal of the European Ceramic Society **16** (1996) 1189–1200

PII:S0955-2219(96)00044-1
0955-2219/96/$15.00

The Influence of Shaping Method on the Grain Size Dependence of Strength in Dense Submicrometre Alumina

Andreas Krell & Paul Blank

Fraunhofer-Institut für keramische Technologien und Sinterwerkstoffe (IKTS), D-01277 Dresden, Germany

(Received 15 August 1995; revised version received 29 January 1996; accepted 8 February 1996)

Abstract

The grain size dependence of the strength of pressureless sintered aluminas is investigated with specimens fabricated by uniaxial pressing, cold isostatic pressing, pressure filtration, gel casting, and combinations thereof. The strength depends on the flaw population, and the observed grain size effect is different with different shaping approaches: with reduced grain sizes the diversity of measured strength averages broadens including increasingly high values for some of the shaping procedures only. Submicrometre grain sizes are, however, not an indispensable prerequisite for a high strength: grain sizes of 1–2 μm are sufficient to achieve 800–900 MPa by pressureless sintering, but present microstructures with grain sizes <1 μm do not indicate a further increase of the strength. Under certain technological conditions, the highest strengths can be associated with a surprisingly small standard deviation. The measured data are discussed considering recent micromechanical investigations of the same materials. Copyright © 1996 Elsevier Science Ltd

1 Introduction

Sintered alumina with its unique combination of high hardness, corrosion resistance, thermodynamic stability and economic advantages is a material that has acquired a wide acceptance in industry. It is used for hip implants, sliding and sealing elements, thread guides, cutting tools, grinding grits and other applications. The typical bending strength of pure and high-quality sintered alumina is about 400–500 MPa after pressureless sintering and in the range of 500–600 MPa in a hot-pressed state.

Riedel *et al.* were among the first who described a pressureless sintered alumina with an improved bending strength of 680 MPa at a grain size of 0·9 μm.[1] Remarkable further progress was achieved during the last years in both processing and properties, but often the best properties result from approaches that are expensive and limit the size and geometrical diversity of the sintered bodies. For example, expensive hot isostatic pressing (HIP) of pure corundum powders gives a strength of about 800 MPa for microstructures with grain sizes between 0·8 and 2 μm;[2,3] after pressureless sintering the strength was about 700 MPa in these experiments.[2] An even higher strength of 908 MPa at a grain size of 1·5 μm was observed when hot-pressing was combined with subsequent hot isostatic pressing.[4] A reported strength of 1300 MPa in a hot isostatically pressed alumina microstructure with 0·8 μm grain size is not clear in all details (in this report, samples with 4–5 μm grain size were measured to give a strength of about 700 MPa which is surprisingly high for such coarse-grained microstructures).[5] It was also observed that even pressureless sintering may produce samples with an average strength of 797 MPa, but a corundum powder with an extremely high sintering activity provided by a very high specific surface of 35 m^2/g was required, and the strength dropped to less than 500 MPa when powders with a surface of 8–22 m^2/g were used.[6] Such a result does not stimulate efforts in pressureless sintering, since processing of powders with high specific surfaces >20 m^2/g is very difficult when macroscopic ceramic bodies with a low frequency of flaws have to be produced under industrial conditions.

On the other hand, until now the properties achieved by novel processing routes that produce complex shapes in combination with pressureless sintering do not compete with the advanced properties given by other approaches. For example, shaping of alumina green compacts by enzyme-catalyzed reactions was performed using an alumina powder with a grain size of 0·5 μm and a specific surface area of 10 m^2/g.[7] As a consequence of difficult dispersion, no strength data that differed significantly from traditional pressureless sintered alumina (i.e. >500 MPa) were reported. Gelcasting, which implies the immediate solidification of a cast

slurry by polymerization of a monomer used as organic binder, seems to be even more difficult: comparing this process for two alumina powders with average particle sizes of 0·5 and 1·5 μm, respectively, the problem of a sufficient degree of dispersion was solved for the coarser one only, and the resulting strength after pressureless sintering was less than 300 MPa.[8]

It is generally assumed that high-purity powders are essential for a high strength (which requires both a sufficiently high fracture toughness K_{Ic} and a small size of the critical flaw at instability). Any subcritical crack growth (usually preceding unstable fracture and increasing the size of the flaw produced on manufacturing) will reduce the strength.[9] Subcritical fracture preferentially follows the grain boundaries because they represent a strong disorder compared with the crystal lattice of the grains, and because subcritical crack growth rates are higher under the condition of disorder (e.g. in amorphous materials, as an extreme).[10] Therefore, impurities that form amorphous grain boundary phases are assumed to prevent a high strength of polycrystalline non-transforming microstructures with equiaxed grains.

Further, it is suggested that a small grain size favours a high strength. The wish physically to understand the influence of the grain size D on the strength $\sigma(D)$ has led to some preference for an Orowan–Petch plot[11,12]

$$\sigma(D) = \sigma_{D\to\infty} + k \cdot D^{-1/2} \qquad (1)$$

where the intercept $\sigma_{D\to\infty}$ has been attributed to microplasticity or residual stress effects, and the analogy with Griffith's theory[13] gives a proportionality of the factor k with the square root of Young's modulus and the work of fracture (k has the dimension of a stress intensity). Often hundreds of data points obtained from different sources have been fitted by such plots without any regard for different processing which must have provided different flaw populations in all these specimens. This neglect of processing is the less convincing since already one of the first analyses[11] reported that different processing of alumina powders (hot pressing and sinter forging) yields plots with different $\sigma_{D\to\infty}$ and k parameters — the very same finding of a grain size effect that depends on processing as will be derived in the present work. There are, however, two more fundamental reasons why an Orowan–Petch plot seems inappropriate: (i) There is no physical basis to describe such different influences as the resistance against microplastic deformation and elastic residual stresses by a single parameter $\sigma_{D\to\infty}$. (ii) At $\sigma_{D\to\infty} = 0$, eqn (1) has to be compared with Griffith's relationship which correlates the strength with the energy of fracture and with a flaw size. Hence, the grain size in eqn (1) needs an interpretation as a defect or at least as a stress concentrator. This may be true when very coarse microstructures are investigated, but it is an improbable assumption for the grain size range between 0·4 and 4 μm discussed here, and even in the intermediate grain size range the experimental evidence of a generally valid $\sigma(D)$ versus $D^{-1/2}$ relationship is poor. For example, a recent treatment that stresses eqn (1) again uses the hypothesis of a proportionality between the grain size and the size of 'pre-existing defects'. To explain that proportionality, the authors associate a flaw size which is 7·5 times the grain diameter with cleavage processes.[14] However, without microscopic evidence for the collective cleavage of many neighbouring grains (which is not a commonly observed phenomenon in fine-grained alumina ceramics) such a hypothesis does not offer a strong argument against the generally accepted idea of technologically caused defects as the fracture origin in most ceramics. In the range between 1·7 and 11 μm, another recent work[15] claims the observation of a linear relationship of strength versus inverse square root of grain size and resumes the idea of peripherically cracked spherical pores with a crack length proportional to the grain size to explain this behaviour. In fact, a least squares fit of their measured data in a double logarithmic plot gives a power of the grain size of –0·29 which is rather different from an inverse square root, and careful fractographic investigations did not present any evidence of the assumed proportionality between a peripherical crack length and the grain size.

It is beyond the scope of the present work to present an alternative theoretical explanation. However, a number of microstructural processes are known with more indirect possible influences of the grain size on strength. For example, small grain sizes promote the visco-elastic relaxation of residual stresses during cooling the sintered microstructures,[16,17] an effect that may reduce grain boundary microflaws[18] and results in an increased resistance against subcritical crack growth. This increase of strength by reduced subcritical crack growth rates due to an increased micromechanical stability of the grain boundaries was demonstrated experimentally by comparing Al_2O_3, ZrO_2(3 mol-% Y_2O_3), Al_2O_3/TiC, and ZrO_2(3 mol-% Y_2O_3)/TiC.[19] However, the actual importance of such an influence in different grain size regions is not clear, and there is no reason to expect that a reduced grain size automatically increases the strength: several investigations indicate that the importance of grain sizes for a high strength can only be discussed in close relationship with the influence of flaws. For example, recent experiments with sintered aluminas representing a broad grain size range of

1–60 μm suggested that under the condition of a fixed technology a grain size effect proportional to the inverse square root of the grain size exists only when the grain size is larger than the typical size of the flaws which initiate failure.[20] Similarly, early systematic measurements with different sintering procedures revealed a trend of different grain size influences depending on the approach of fabrication,[11] i.e. depending on the different flaw populations. Therefore, it is evident that a low frequency of small flaws cannot be achieved by simply sintering a highly pure, extremely fine-grained powder at low temperatures (avoiding grain growth and producing a microstructure with submicrometre grain size). This feature is illustrated by a comparison of two investigations which used an identical alumina powder† and similar shaping procedures (cold isostatic pressing) but nevertheless showed quite different hardness values of about 19 and 22 GPa at similar grain sizes of 0·85 and 0·65 μm, respectively.[21,22] Also, the bending strength was lower than 400 MPa in the first report. Obviously, the potential advantages of very fine-grained powders with respect to lower sintering temperatures are opposed by additional difficulties in shaping when a high homogeneity and a low frequency of defects in the green (unsintered) body are required. This difficulty is not restricted to individual technologies, and there is no approach that generally might avoid this problem. For example, reduced powder grain sizes between 2·5 and 0·05 μm were observed to be accompanied by increasing agglomeration and reduced green densities even under the condition of careful pressure filtration with a preceding ultrasonic treatment of the aqueous slurry at low pH $\approx$2–4 (where the electrochemical surface potential of alumina and repulsive forces are high).[23] On solid state sintering, these agglomerates have a twofold detrimental effect: locally different shrinkage rates in more and in less dense subregions increase the size of flaws (between agglomerates), and the elimination of associated porosity (with a large size of these defect-like pores) requires an increase of the sintering temperature and promotes grain growth.[24]

The present work was intended to investigate the influences of the grain size on the strength of pressureless sintered alumina ceramics for a range of different processing approaches. All of the investigated technologies had been optimized first to minimize the probability of accidental results where the strength would be determined by different control of processing, and only the final results of these optimizations are given here. It is, of course, obvious that any 'optimization' is temporary, and further improvements are probable. It was another objective to compare possible grain size effects with recent micromechanical studies on these and similar materials.

2 Materials and Methods

Powder technology with aqueous slurries was used to produce pressureless sintered alumina bodies with relative densities in a narrow range of 99·2 ± 0·4%; the densities were measured following Archimedes' principle and related to a theoretical density of 3·9865 g/cm^3. Most batches were prepared with a high-purity alumina powder Taimicron TM-DAR‡. In a first step, it was dispersed in distilled water with an organic dispersant and, for batches that were freeze dried, with a binder solution of polyvinyl alcohol and glycerin. With few exceptions given below, all specimens were sintered in air for two hours. Different powder processing resulted in green bodies with different packing homogeneity, requiring different sintering temperatures to achieve the desired density which was then associated with different grain sizes (grain sizes were determined by linear interception: average grain size D = 1·56 × average linear intercept). Hence, the characteristic differences of the approaches will be described here, but it is not intended to discuss details of the technology and of the microstructural development in the present paper.

With Taimicron-DAR, uniaxial pressing required a high sintering temperature (1450°C) to achieve a relative density of about 99%. Bars were formed at a pressure of 200 MPa with a freeze-dried slurry that had been homogenized in an attrition mill for one hour at 1000 rev/min. The relative green density obtained was 57·3%. The high sintering temperature produced an average grain size of 1·25 μm. These specimens were compared with the strength results of coarser microstructures (grain size 2·8 μm) fabricated previously by the same shaping procedure but using A16# as the raw powder, doped with 0·14 wt% MgO (introduced as a solution of $MgCl_2 \cdot 6H_2O$), and sintered at 1590°C for 2·5 hours in air.

Uniaxial pressing of plates (60 × 60 × 7 mm^3) at 50 MPa followed by cold isostatic pressing (CIP) at 700 MPa increased the green density with Taimicron-DAR to 60% and reduced the required sintering temperature by 50 K (to 1400°C). After

†Taimei CHBS Chemicals, Tokyo, Japan, average grain size 0·2 μm, specific surface (BET) 14 m^2/g, >99·99% Al_2O_3.

‡Taimei CHBS Chemicals, Tokyo, Japan, average grain size 0·2 μm (about 75 wt% smaller than 0·4 μm), specific surface (BET) 14 m^2/g, >99·99% Al_2O_3.

#Alcoa, Bauxite, AR, USA, average grain size 0·6 μm (about 75 wt% smaller than 0·8 μm), specific surface (BET) 9·5 m^2/g, >99·9% Al_2O_3.

sintering, bars were cut from the cold isostatically pressed bodies. Compared with uniaxial pressing, CIP samples exhibited a significantly reduced grain size of 0·65 μm; almost equal microstructures and strength data were obtained with reduced pressures of 30 MPa (uniaxial) combined with 350 MPa (CIP). With MgO doping (0·1 wt% added as an $Mg(NO_3)_2$ solution), application of ultrasonically assisted dispersion, and a vacuum de-gassing of the slurry it was possibly to produce green bodies that sintered to a density of 99·0% at 1275°C, but both the microstructure and the strength remained approximately constant. Again, comparative experiments were performed with a coarser microstructure (4·5 μm) fabricated by cold isostatic pressing of A16 powder and sintered at 1620°C for one hour.

Pressure filtration of binder-free slurries on a 0·1 μm membrane at a pressure of 20 bar was preceded by an ultrasonically assisted dispersion of the 0.2 μm powder. Slow drying was required to get samples with a low flaw density. The green density was 66%. Sintering at 1300°C yielded a relative density of 99.0% and an average grain size of 0·59 μm.

Further progress towards smaller grain sizes was achieved by cold isostatic pressing of the green bodies after pressure filtration: after sintering at 1300–1350°C the grain size was 0·4 μm. Differences in details of the processing approach caused a different packing homogeneity of the green bodies and required different sintering temperatures between 1300 and 1400°C. In this way, microstructures with grain sizes up to 4 μm were produced. No significant influence of MgO doping was observed with respect to microstructures or properties.

Aqueous gel casting was performed with a monomer combination of acrylamide (AM) and *N,N'*-methylene-bis-acrylamide (MBAM) described by Young *et al.*[8] Tested monomer concentrations (sum of AM and MBAM related to alumina) were 3·8 and 7·4 wt%, the weight ratio of AM : MBAM was 24 : 1. Before polymerization, the powder in the slurry was carefully dispersed for 0·5 and 2 hours, respectively. Ammonium persulfate was added as initiator. After casting, the molds were immediately placed into a drying chamber under slight vacuum (200 mbar). The chamber was then filled with nitrogen to avoid oxidation, and the temperature was raised to 60°C for one hour. No catalyst was added to accelerate the polymerization. The molds were kept under nitrogen for 8–10 hours after polymerization was finished. The subsequent drying procedure was the same as applied following pressure filtration. One of the gelcast batches was additionally cold isostatically pressed (called batch 2 below).

Casting and pressure filtration are approaches that may give rise to some cooperative alignment of powder particles and to mutual orientation effects which can be assumed to contribute to reduced residual microstresses and to the strength. No detailed X-ray studies were performed to exclude such effects, but a careful scanning and transmission electron microscopy of the raw materials did not reveal any morphological features that might make the powders liable to alignment. Also, X-ray investigations to measure residual microstresses[17] did not give indications of a preferential orientation in the sintered microstructures.

With the large body of fractographic investigations published during the past 20 years it is obvious that such studies can distinguish typical types of flaws that act as an origin of fracture (e.g. defects in the volume of hot-pressed Si_3N_4 but mostly surface and corner flaws in both pressureless sintered and in hot-pressed Al_2O_3 associated with stress corrosion in the latter material in the presence of (humid) air[25]). However, on the rough fracture surfaces it is often very difficult to identify the individual (one?) flaw that initiated failure, and subcritical crack growth frequently obscures the borders (the size) of the flaws. Also, little is known about a statistical analysis of the frequency of flaws per volume unit by fractographic means in ceramics (contrary to some efforts in glasses). Since the question addressed here is focused on the parameters of typically observed strength distributions and does not concern the flaw characteristics of an individual specimen with a given (measured) strength and toughness, the search for flaws on fracture surfaces would promise less insight than the investigation of the volume of the samples, e.g. by investigating the elastic response (which did not reveal significant differences) or by analysing carefully polished cross-sections. A frequency of flaws (FF) was determined by counting all defects $\geq$0·3 μm (different kinds of pores, crack-like flaws). Additionally, a dimensionless flaw 'density' ρ_{fl} that considers both the frequency and the size distribution of defects as observed on polished and thermally etched cross sections was measured using a definition introduced previously for the characterization of microcracks in zirconia-toughened alumina:[26]

$$\rho_{fl} = \frac{\sum l_i^2}{A} \tag{2}$$

where l_i are the apparent maximum lengths of flaws seen on a polished cross-section, and A is the analysed area. In previous studies, this definition provided the best correlation between the microcrack density and the mechanical behaviour compared with other treatments of a given size distribution of microcracks.[27] Probably, this advantage has to

be attributed to the strong impact of larger flaws caused by the square in eqn (2). It is suggested here that this measure might also describe a statistical correlation of flaws observed in the volume of sintered alumina specimens with their strength.

All specimens were ground in the direction of their axes on four sides (to a cross-section of 3×4 mm^2) and chamfered with a resin-bonded diamond wheel of 40–50 μm grain size at a feed rate of 0·01 mm per cut. The strength was measured in three-point-bending with a 24 mm span and with a cross-head velocity of 0·5 mm/min; the load-bearing pins of the jig were free to rotate around and to slide along their axes to minimize frictional effects. Vickers indentations at a load of 98·1 N (10 kgf) were used to measure the indentation toughness K_{Ic} (formula (4) derived by Anstis *et al.*[28] was applied with a parameter $\S_V^R = 0{\cdot}023$ that results from their fitting plot for the Al_2O_3 ceramics investigated there). To test the reliability of the resulting K_{Ic}, some of the batches were chosen for comparative strength-in-bending[29] measurements. No significant difference was observed between the results of the two methods. In each single experiment the average was determined from 5–8 specimens; the typical standard deviations of σ_f and K_{Ic} were ±7–10% with some exceptions that will be discussed separately.

The Young's modulus was derived from the measured resonance frequency. However, all results were quite similar and in the range between about 370 and 390 GPa. No conclusions about the flaw populations could be drawn from the small differences observed.

Careful experiments to study subcritical crack growth kinetics with short cracks (stable fracture of bending bars) revealed significant differences when different materials were compared,[19] but it was not possible to resolve the different kinetics in sintered aluminas of different quality. Another shortcoming is the expense in performing tests with the stable fracture of macroscopic bars which actually makes statistically substantiated results impossible. Therefore, here it was attempted to get a qualitative measure of subcritical crack propagation by comparing the time-dependent growth of indentation cracks in air. Generally, this kind of experiment depends on the driving force that arises from the residual stress at the indentation and does not relax significantly on unloading. However, the value of such investigations is limited when in air most of the subcritical growth occurs immediately after unloading before the first measurement can start. To avoid this problem, the crack length was measured three times: at t_0 immediately after indentation, at t_1 six weeks later, and at t_2 six months after indentation. With a crack length 2c, the observed scatter in the subcritical growth increment $\Delta(2c) = 2c(t_2)-2c(t_1)$ was much less than for the time interval t_1-t_0. Hence, only the results for the growth between t_1 and t_2 are reported here.

With an indentation load of 98·1 N, the typical crack lengths were in the range of 100–200 μm which is 'short' compared with the crack length in precracked bending bars but large compared with typical flaw sizes in high-strength ceramics. In spite of the probable absence of R-curve effects in the fine-grained microstructures investigated here the degree of a possible equivalence in the behaviour of the indentation cracks compared with the growth of shorter flaws is unknown, and any interpretation should be done with care.

Individual samples from batches that represent the whole range of shaping procedures and grain sizes were chosen for this investigation; the number of analysed indentation cracks was about 10–20 in each test. The average crack growth rates were 3×10^{-12} m/s–13×10^{-12} m/s in the first period $t < t_1$ and dropped to $0{\cdot}3 \times 10^{-12}$ m/s–$2{\cdot}3 \times 10^{-12}$ m/s when for $t_1 < t < t_2$ the crack tip proceeded to more distant regions with lower residual stress.

3 Results

Figure 1 compares the influence of different shaping approaches and of the associated green densities on the temperature effect in densification on sintering (2 h, air). Whereas there is no significant effect of the observed green densities, a great shift to lower isothermal sintering temperatures is achieved by the choice of a proper shaping procedure.

The strength results are given in Fig. 2; straight lines represent least square fits calculated for the different shaping approaches. Figure 2 also provides an immediate comparison of the grain size effects

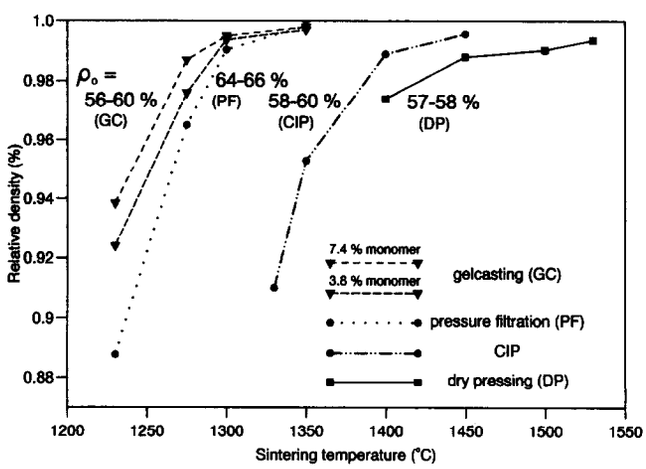

Fig. 1. Influence of shaping approaches and of the associated green densities on the temperature effect in densification on isothermal sintering (2 h, air). All experiments performed using the same corundum powder TM-DAR.

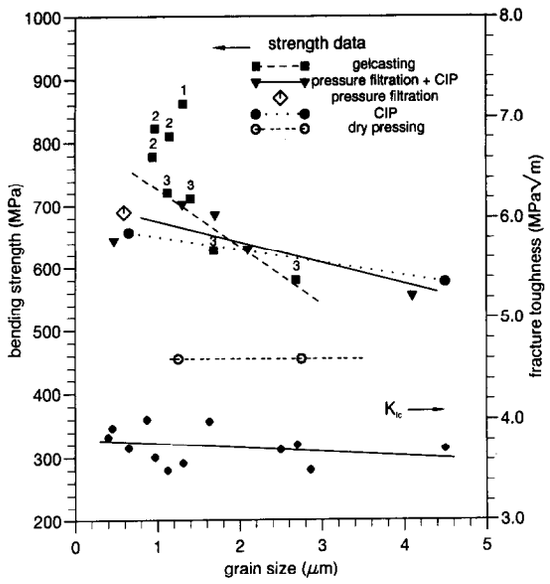

Fig. 2. Grain size and technology effects in the strength and toughness of pressureless sintered alumina. Each data point represents the averages of grain size and strength measured for a group of specimens sintered at the same temperature. The numbers that distinguish different gel casting routes refer to Table 1, different data points for one casting route refer to microstructures sintered at different temperatures.

(the slopes) in strength and toughness. For this end, the axes of strength and toughness are defined such that equal percentages of variations in both properties give approximately equal slopes. It is important to emphasise that each data point in Fig. 2 is an average value of a group of fractured specimens: due to the high number of tested individual specimens, the reliability of the given grain size effects is high even when the slopes are very small. For example, the confidence that the slopes for toughness or for the strength of samples prepared by pressure filtration (+ CIP) are different to zero is higher than 99·9%! Different shaping procedures by gelcasting were tested and are distinguished in Fig. 2 by numbers; results of larger grain size variations are given for batch 3 only, and the least squares fit includes only the data for this batch.

In agreement with recently published results for the special case of isostatically shaped and hot isostatically sintered (pressure 100 MPa) high-purity alumina materials,[14] Fig. 2 shows a grain size effect in the strength which for most of the investigated technological approaches cannot be explained by the almost constant toughness. Obviously, the general trend of increasing strength at reduced grain size is quite different depending on the applied shaping technology. No submicrometre grain size is required to produce pressureless sintered alumina bodies with a high strength of 800–900 MPa. As shown by the example of gelcasting in the grain size range of 1–1·3 μm, relatively small variation of the dispersion procedure within the narrow limits of one technological framework can provide a substantial increase of the strength at almost constant grain size. Table 1 compares microstructures produced by three different gelcasting procedures for the special case of sintering conditions that resulted in similar grain sizes of about 1·15 ± 0·15 μm. The duration of slurry dispersion and differences in the monomer concentration did not affect the sintering temperatures (1275–1300°C) and the grain sizes (1–1·3 μm), but the strength was increased significantly by the improved dispersion. Table 1 suggests that probably both the average strength and the strength distribution are strongly affected by such technological changes. The small standard deviation given in Table 1 for batch 2 at an average grain size of about 1 μm would represent a Weibull modulus of 40–50, but the numbers of specimens in the present investigations are too small to draw final conclusions about the statistics of the observed strength behaviour.

With the strong impact of powder processing demonstrated by Fig. 2, a closer inspection of flaw populations becomes necessary. Figures 3–6 show typical, thermally etched microstructures. Probably, the crack-like flaws in dry-pressed and in cold isostatically pressed samples are relicts from hard granules (Fig. 3a, Fig. 4a). Hence, no such defects exist in the microstructures produced by the wet shaping techniques (pressure filtration (Fig. 5), gel casting (Fig. 6)). Counting all defects >0·3 μm, the frequency of flaws is given in Table 2. In a conventionally dry-pressed microstructure with a strength of 400 MPa this flaw frequency is about two orders of magnitude higher than in the gelcast batch 1 with a strength >800 MPa or in batch 2 with its extremely small standard deviation (Table 1). A similar correlation is obtained with the microflaw density ρ_{fl} that additionally incorporates the size distribution of the flaws: it drops to about 1% when a dry-pressed batch is compared with high-strength gelcast bodies (Table 2).

Table 1. Strength data of gelcast aluminas after pressureless sintering

Batch number	*Monomer content (wt%)*	*Duration of slurry dispersion (min)*	*Grain size (μm)*	*Average strength (MPa)*	*Standard deviation (MPa)*
1	3·8	130	1·31	862	±102
2	7·4 (+CIP)	130	0·97	822	±19
3	3·8	40	1·12	720	±47

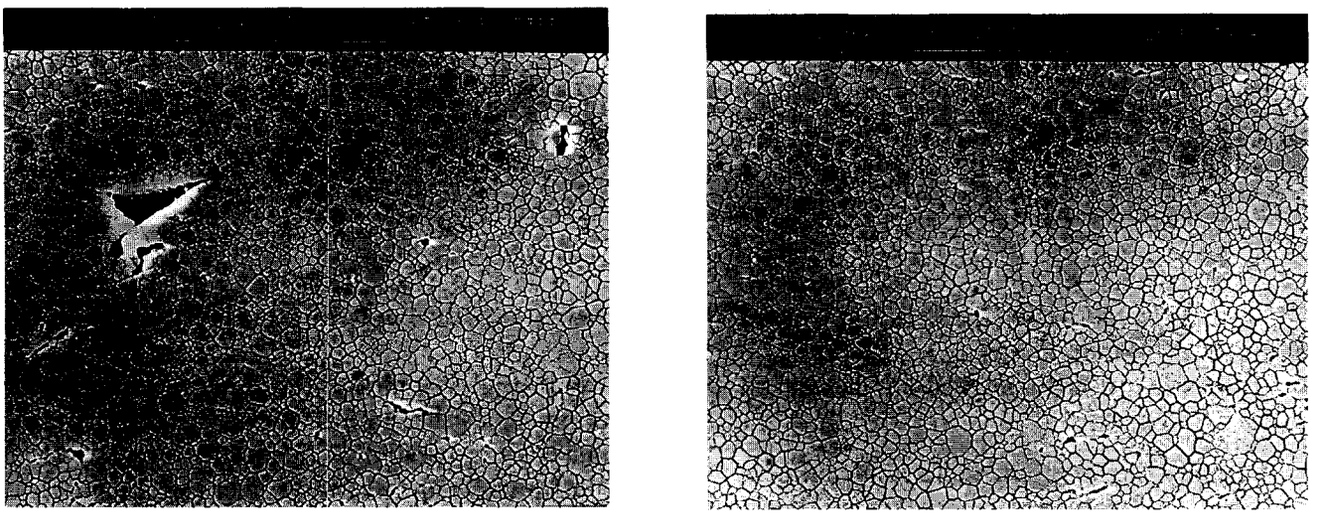

Fig. 3. Heterogeneous flaw distribution in a dry-pressed microstructure sintered at 1450°C. Average grain size 1·25 μm, average strength of this batch 400 ± 60 MPa. (a) Large pores and crack-like flaws, (b) subregion with small flaws only.

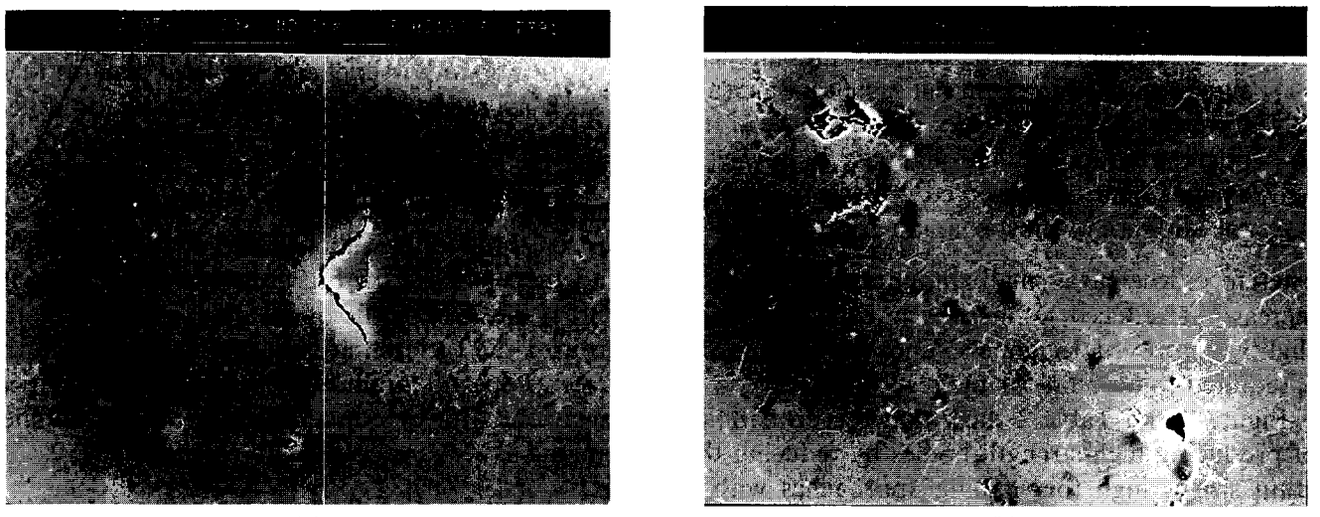

Fig. 4. Smaller defects in alumina bodies fabricated by cold isostatic pressing and sintering at 1400°C. Average grain size 0·65 μm, average strength of this batch 635 ± 32 MPa. (a) Crack-like flaw, (b) pores ≤ grain size.

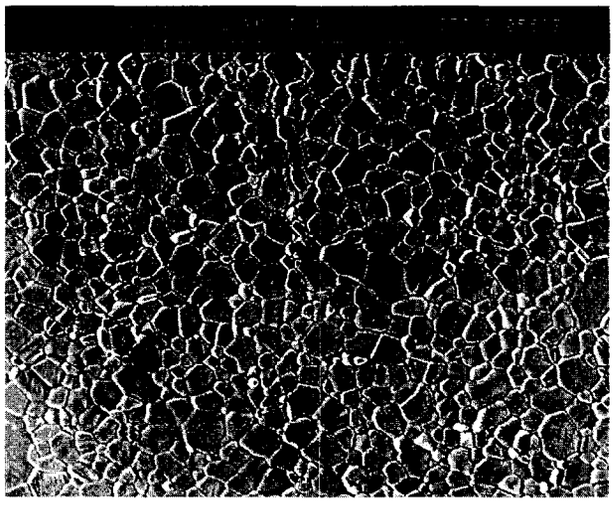

Fig. 5. Homogeneous microstructure: pressure filtration and sintered at 1300°C. Average grain size 0·59 μm, average strength of this batch 689 ± 63 MPa.

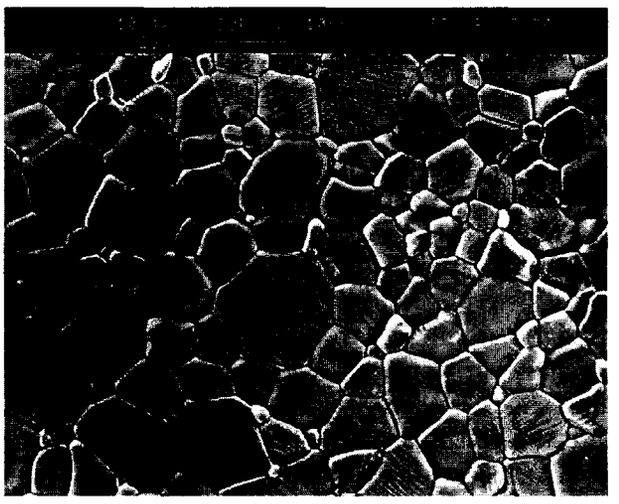

Fig. 6. Gelcast batch 1 (cp. Table 1) sintered at 1300°C. Average grain size 1·31 μm, average strength of this batch 862 ± 102 MPa.

Table 2. Frequency of flaws ≥0·3 μm (FF) and microflaw density ρ_{fl} defined by equation (2)

Shaping approach	*Bending strength (MPa)*	*Grain size (μm)*	*Frequency of flaws FF (10^9 m^{-2})*	*Flaw density ρ_{fl} (10^3)*
Gel casting 1	862 ± 102	1·31	0·7	1
Gel casting 2 (+CIP)	822 ± 19	0·97	0·2	4
Dry pressing	400 ± 60	1·25	50	96

Figure 2 also addresses the question whether the observed variations in strength can be attributed to grain size or technological influences on the fracture toughness:

- Unlike the strength, there is no influence of different processing routes on the toughness, and all data can be described by one least squares' fit.
- Whereas the influence of the grain size on K_{Ic} is so small that none of the measured averages is significantly distinguished from another when individual averages of data sets are compared, the least squares' fit that incorporates all measurements shows a slight but significant increase towards smaller grain sizes. The influence of the microstructure on the toughness is, however, smaller than the observed grain size effect in the strength of most shaping approaches.

Therefore, whereas a small amount of the strength increase at reduced grain sizes is explained by a slightly improved toughness, another mechanism is required to account for the rest.

Figure 2 and Table 2 show that the probability of producing high-strength bodies by reducing the grain size is high for shaping approaches with a potential to give low flaw densities. As suggested in the introduction, reduced subcritical crack growth might explain this observation. However, if some of the strength increase is caused by the toughness, the subcritical effect does not need to be very strong, and stable indentation crack growth had to be assessed for a long time to get measurable results. The lower part of Fig. 7 shows the measured subcritical growth of indentation cracks (testing load 98·9 N) for the time interval t_1 = six weeks → t_2 = six months. As expected, the least squares approximation in Fig. 7 correlates growing subcritical crack elongation with decreasing strength and vice versa. The upper part of Fig. 7 gives the average strength–grain size relationship of those eight batches that were selected for the subcritical measurements. To compare with the following Fig. 8, here the full line is a least squares plot resulting from a linear regression analysis of these eight data points in Fig. 7. To make the comparison with Fig. 2 easier, the broken and the dotted lines in Fig. 7a are the same least squares fits for gelcasting and for cold isostatic pressing as already given in Fig. 2.

With Fig. 8, a plot of the subcritical crack elongation versus the grain size was derived to compare whether the (shaping-influenced!) increase of the strength with reduced grain size in Fig. 2 (and Fig. 7) was really associated with a grain-size effect in subcritical crack propagation. However, whereas more than 150 samples were required to derive the grain size–strength result in Fig. 2, the subcritical tests had to be restricted to a much smaller number. Hence, a proper analysis of possible influences of the shaping procedures on the subcritical crack growth was impossible, and the least squares fit in Fig. 8 averages over samples produced by different approaches. Therefore, the slope cannot be compared with any of the slopes in Fig. 2 but with the slope of the full line in Fig. 7a which characterizes these eight subcritically analysed samples and their batches. In Fig. 8 the measurements 5/6 (CIP), the average fit of all data points, and the group 1–3/7 (gelcasting) indicate an increase of the larger slope for grain-size effect in the subcritical behaviour with the same *technologically* determined ranking as seen in the strength results of Fig. 2.

4 Discussion

The technological background of the different strength–grain size relationships in Fig. 2 and of the different flaw populations demonstrated by Figs 3–6 and Table 2 is, of course, the role of the applied shaping approaches. The data on green densities and sintering in Fig. 1 clearly show that it is really the microstructural homogeneity of the 'green' samples and not simply the green density that dominates the performance: there are differences in the green densities, but just the limiting examples — gel casting and dry pressing — exhibit quite similar green densities which cannot explain the very different densification on sintering. With the identical powder used for all experiments in Fig. 1, the one explanation is a greatly improved homogeneity in the sequence dry pressing, cold isostatic pressing, pressure filtration and gelcasting. With this understanding of the microstructural homogeneity — i.e. the absence of flaws —

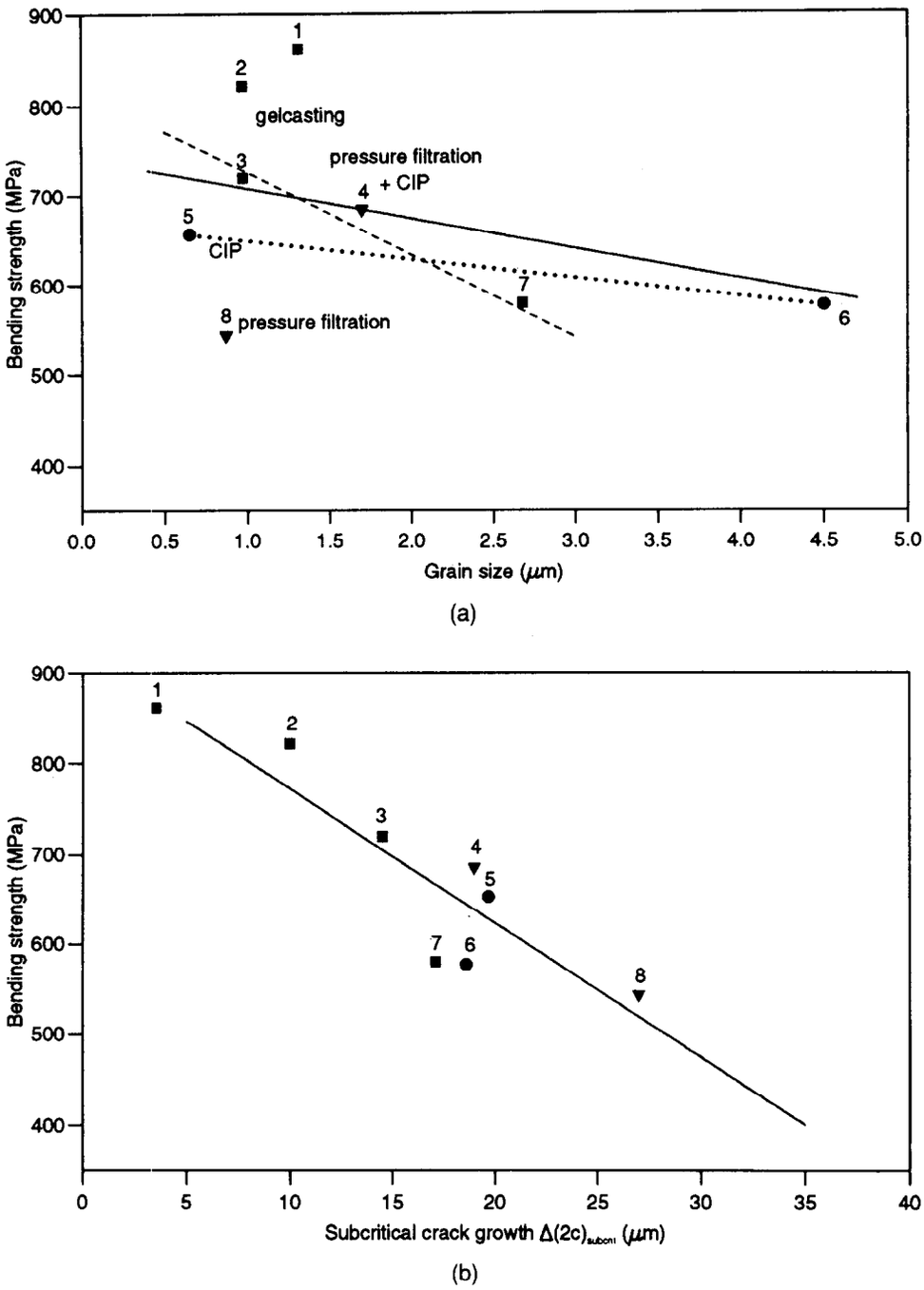

Fig. 7. Strength–grain size relationship (a) and subcritical growth of radial indentation cracks (b) of sintered batches selected from Fig. 2. Straight lines are least squares fits. Strength ranking numbers associate specimens in (b) to batches in graph (a), numbers 1–3 are consistent with Table 1 and Fig. 2.

in the green bodies as the reason of the extremely low sintering temperature of the gelcast samples, it is not surprising to find a low frequency of flaws also in the sintered microstructures (Table 2) and an extremely high strength associated with a very small standard deviation (Table 1, batch 2: high monomer content, + CIP).

The observed trend of an increasing strength at reduced grain size is consistent with other investigations which, on the other hand, also confirm that under constant technological conditions the grain-size effect is small in the grain-size range less than 5 μm.[20] The strongest influence observed in the present experiments (gelcast batch 3) is of the same order as, for example, described for Al_2O_3/Ti(C,N) composites with grain sizes between 0·5 and 2 μm.[30] Actually, the grain-size effect documented in Fig. 2 is small for most of the batches, and the most important conclusion is that within the range investigated, reducing the grain size in the absence of other processing changes does not constitute a useful means of developing high-strength sintered alumina products. For example, a previous report[21] used the same raw material, and an essentially equal shaping procedure (CIP), and arrived at a similar submicrometre grain size

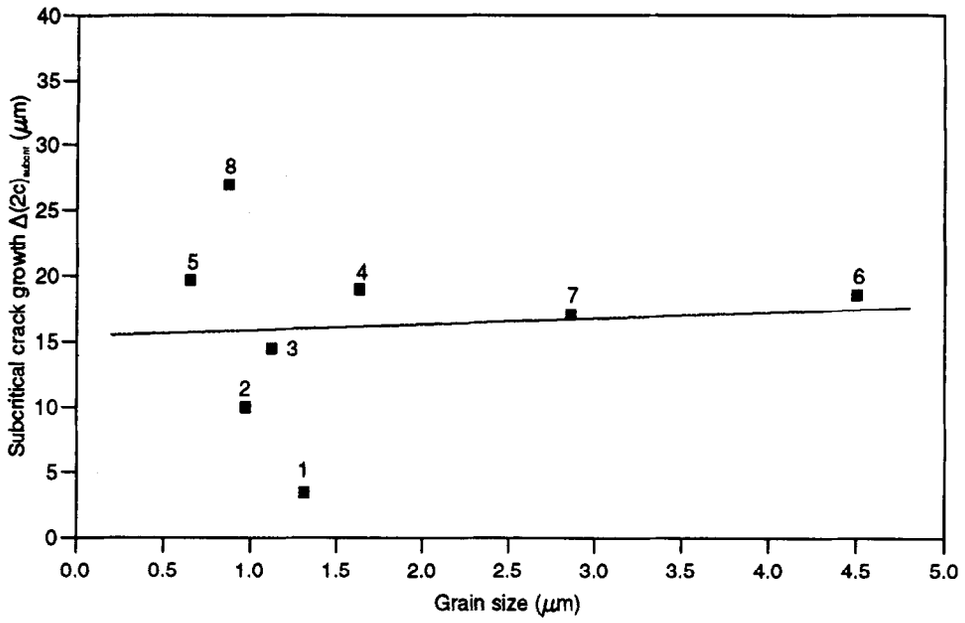

Fig. 8. Subcritical growth of radial indentation cracks versus grain size for the time interval between six weeks and six months after indentation. The straight line is a least squares fit. Strength ranking numbers are identical with Fig. 7.

of 0·8 μm — but the maximum strength was only 380 MPa compared with 660 MPa at 0·65 μm in the present work. The one way to understand these differences is to analyse the flaw structures. Figure 2 and Figs 3–6 together with the observed correlation of flaw densities and strengths (Table 2) demonstrate that the most powerful tool is to develop shaping and sintering procedures that avoid larger defects.

Reduced grain sizes are essential for a high hardness,[22] but they only assist efforts to increase strength or toughness (Fig. 2). Additional mechanisms other than the stress concentration at flaws and the effect of the fracture toughness are probably contributing to the observed high strength of advanced pressureless sintered aluminas and may introduce the observed effects of grain sizes. In analogy with the explanation of the improved wear resistance of sintered fine-grained alumina which is caused by reduced grain pull out,[31] it is suggested that a small grain size and the associated reduced residual stress level may correlate with more perfect grain boundaries and with reduced subcritical growth of the flaws. In fact, reduced subcritical crack growth has been observed to give smaller flaw sizes at instability associated with an increased strength in sintered alumina,[25] zirconia,[19] and in TiC-reinforced oxide ceramics.[10,19] The present results in Fig. 7 strongly support the idea of reduced flaw sizes by decreased subcritical crack growth. Certainly, together with the 6% increase in K_{Ic} for the grain-size range investigated here (Fig. 2) the moderate grain-size effect in the subcritical crack growth data in Fig. 8 (+12%) is too small to explain the 29% strength increase of the investigated batches (Fig. 7). However, with the strong evidence of a shaping influence on the grain-size effect in strength from Fig. 2, the selection of samples from only eight different batches for the subcritical studies imposes significant limitations as to the significance of the fit in Fig. 8, and the real effect may be stronger as indicated by the fit. For example, the gelcast samples 1–3 and 7 suggest a strongly reduced subcritical crack growth at decreasing grain size — a behaviour which compares well with the strong grain-size effect in the strength of only the gelcast batches in Fig. 2 and which may correlate with the fact that with the apparent absence of larger flaws in gelcast microstructures (Fig. 6) defects able to initiate fracture need subcritical growth for their formation. Further, the grain-size influence on subcritical crack growth may depend on the crack propagation rate and may be different at other crack growth velocities than the about 10^{-12} m/s assessed here. On the other hand, the limited significance of the data in Fig. 8 should not be used for extended speculations, and additional subcritical measurements with an expenditure of samples comparable with the strength analyses in Fig. 2 are obviously required to confirm the observed trend of a grain-size effect in the slow growth of flaws.

It is not clear whether this potential ability to increase the strength by reducing the grain size into the region of 1–2 μm will hold in the submicrometre range as well. In the present investigations, none of the tested technological approaches resulted in a significantly improved strength when the grain size was reduced from about 1–1·5 μm to less than 1 μm, and a similar trend was

observed in hot isostatically pressed alumina where a grain-size reduction from 1·1 to 0·8 μm caused a slight drop of the average strength from about 825 to 775 MPa.[14]

New shaping approaches do not only result in an average strength that is twice the level known for conventional alumina or for previous gelcasting results. The measured low frequency of flaws in the high-strength gelcast batch 2 with its small standard deviation of about ±2% indicates that a very high reliability can be achieved in spite of an only moderate toughness if appropriate technologies are developed, but more data with larger series of samples are required to draw valid conclusions about the statistical mechanical behaviour. Nevertheless, the great progress from previously published strength data for gelcast alumina to the present results demonstrates the high potential of this shaping approach.

5 Conclusions

High-purity alumina exhibits an increasing potential for higher strengths at decreasing grain sizes. In advanced high-strength materials, the grain-size effect of the strength is stronger than the slight increase of the toughness. Surprisingly, maximum strength averages were obtained with grain sizes of 1–1·5 μm; contrary to hardness[22] and wear resistance,[31] there was no indication of a further strength improvement in the submicrometre range.

It depends on the flaw population whether this *potential* for a high strength can be exploited or not: the actual significance of the grain-size effect on strength depends on the applied processing, shaping, and sintering approaches. There is a correlation of increasing strength and reduced subcritical crack growth in finer-grained alumina microstructures, but with grain sizes between 0·4 and 4 μm the contribution of defect-avoiding technologies to the achieved increase in strength generally seems to be more important than the pure grain-size effect. With a fixed technology, a decrease of the grain size from the range of 2–5 μm to 0·4–1·5 μm never increased the strength by more than about 150 MPa. On the other hand, technological improvements increased the strength of pressureless sintered bars to more than 800 MPa which is about 400 MPa above the conventional level of high-quality aluminas. With sufficient dispersion, wet-shaping techniques are most promising to reduce the flaw density independent of the different applied approaches (pressure filtration, gel casting).

A reduced flaw density is assumed to be the most effective tool to improve the reliability of pressureless sintered alumina bodies. The results indicate a chance for both a high average strength of more than 800 MPa and a very small standard deviation that represents a Weibull modulus of about 40–50. Such strength properties together with the high hardness,[22] wear resistance[31] and thermodynamic (i.e. oxidative and corrosive) stability will make these advanced alumina ceramics attractive for both well-known and new fields of applications.

Acknowledgments

The investigations have been supported in part by the Deutsche Forschungsgemeinschaft under contract Kr 1398/1-1.

References

1. Riedel, G., Bürger, W., Chylek, S. & Vrbacky, I., Feinkristalline, niedrigsinternde Korundkeramik (Fine crystalline corundum ceramics sintered at low temperature, in German). *Silicates Ind.*, **54** (1/2) (1989) 29–35.
2. Mizuta, H., Oda, K., Shibasaki, Y., Maeda, M., Machida, M. & Oshima, K., Preparation of high-strength and translucent alumina by hot-pressing. *J. Am. Ceram. Soc.*, **75** (1992) 469–73.
3. Hayashi, K., Kobayashi, O., Toyoda, S. & Morinaga, K., Transmission optical properties of polycrystalline alumina with submicron grains. *Mater. Trans.*, **32** (1991) 1024–9.
4. Staehler, J. M., Predebon, W. W. & Pletka, B. J., High strength alumina and process for producing same. Patent Application US-5 352 643, Int. Class. C04B35/10, published 4 Oct 1994.
5. Takahashi, T., Katsumura, Y. & Suzuki, H., Cutting performance of white ceramic tools having high strength (in Japanese). *J. Japan. Soc. Powder & Powder Metall.*, **41** (1994) 33–7.
6. Rajendran, S., Production of ultrafine alpha alumina powders and fabrication of fine grained strong ceramics. *J. Mater. Sci.*, **29** (1994) 5664–72.
7. Graule, T. J., Baader, F. H. & Gauckler, L. J., Shaping of ceramic green compacts direct from suspensions by enzyme-catalyzed reactions. *cfi/Ber. Dt. Keram. Ges.*, **71** (1994) 317–23.
8. Young, A. C., Omatete, O. O., Janney, M. A. & Menchenhofer, P. A., Gelcasting of alumina. *J. Am. Ceram. Soc.*, **74** (1991) 612–16.
9. Krell, A. & Pompe, W., The influence of subcritical crack growth on the strength of ceramics. *Mater. Sci. Eng.*, **89** (1987) 161–8.
10. Krell, A. & Seidel, J., Hochfeste Keramiken auf Al_2O_3-Basis durch kontrollierte Korngrenzenstrukturen (High-strength ceramics on the basis of Al_2O_3 by controlled grain boundary structures, in German). *Fortschrittsber. der Dt. Keram. Ges.*, **9** (1994) 138–57.
11. Rice, R. W., Strength/grain-size effects in ceramics. *Proc. Brit. Ceram. Soc.*, **20** (1972) 275–97.
12. Carniglia, S.C., Reexamination of experimental strength-vs-grain-size data for ceramics. *J. Am. Ceram. Soc.*, **55** (1972) 243–7.
13. Griffith, A. A., The phenomena of rupture and flow in solids. *Philos. Trans. Roy. Soc. (London)*, **221A** (1920–21) 163–98.
14. Miyahara, N., Yamaishi, K., Mutoh, Y., Uematsu, K. & Inoue, M., Effect of grain size on the strength and

fracture toughness in alumina. *JSME International Journal*, **A37** (1994) 231–7.
15. Seidel, S., Claussen, N. & Rödel, J., Reliability of alumina ceramics: Effect of grain size. *J. Europ. Ceram. Soc.*, **15** (1995) 395–404.
16. Blendell, J. E. & Coble, R. L., Measurement of stress due to thermal expansion anisotropy in Al_2O_3. *J. Am. Ceram. Soc.*, **65** (1982) 174–8.
17. Krell, A., Teresiak, A. & Schläfer, D., Grain size dependent residual microstresses in submicron Al_2O_3 and ZrO_2. *J. Europ. Ceram. Soc.*, **16** (1996) 803–11.
18. Krell, A. & Pompe, W., Grain boundary microdamage due to visco-elastic relaxation of residual stresses in alumina ceramics. *Phys. Stat. Sol. (A)*, **111** (1989) 109–17.
19. Krell, A., Grain boundary relevant micromechanical investigations and microstructural observations in ZrO_2 ceramics. In *Proc. 3rd Conf. of the Europ. Ceram. Soc., Vol. 3*, ed. P. Duran & J. F. Fernandez. Faenza Editrice Iberica, San Vicente, 1993, pp. 489–94.
20. Koyama, T., Nishiyama, A. & Niihara, K., Effect of grain morphology and grain size on the mechanical properties of Al_2O_3 ceramics. *J. Mater Sci.*, **29** (1994) 3949–54.
21. ZumGahr, K.-H., Telle, R., Zimmerlin, B. & Park, S.-H., Einfluß der Korngröße auf mechanische Eigenschaften und den ungeschmierten reversierenden Gleitverschleiß von Al_2O_3-Keramik (Influence of grain size on mechanical properties and the unlubricated fretting wear of Al_2O_3 ceramics, in German). *Materialwiss. und Werkstofftechnik*, **23** (1992) 329–38.
22. Krell, A., Grain size dependence of hardness in dense submicron alumina. *J. Am. Ceram. Soc.*, **78** (1995) 1118–20.
23. Nienburg, N., Stein, P. & Harbach, F., Nasse Formgebung von feinkörnigen homogenen α-Al_2O_3-Keramiken (Wet shaping of fine-grained homogeneous α-Al_2O_3 ceramics, in German). *cfi/Ber. Dt. Keram. Ges.*, **66** (1989) 189–97.
24. Lange, F. F., Sinterability of agglomerated powders. *J. Am. Ceram. Soc.*, **67** (1984) 83–9.
25. Kim, B.-N. & Kishi, T., Fractography of Al_2O_3 ceramics strengthened by precoarsening treatments. *J. Ceram. Soc. Japan (Int. Edn.)*, **102** (1994) 1155–9.
26. Krell, A., Blank, P. & Weiss, T., Influence of microcracking and homogeneity on the mechanical behaviour of (Al_2O_3 + ZrO_2) ceramics. *J. Mater. Sci.*, **22** (1987) 3304–8.
27. Krell, A. & Schulze, D., Quantitative Untersuchungen von Mikrorißstrukturen in gesintertem Aluminiumoxid (Quantitative assessment of microcrack structures in sintered alumina, in German). *Silikattechnik*, **36**(12) (1985) 294–6.
28. Anstis, G. R., Chantikul, P., Lawn, B. R. & Marshall, D. B., A critical evaluation of indentation techniques for measuring fracture toughness: I, Direct crack measurements. *J. Am. Ceram. Soc.*, **64** (1981) 533–8.
29. Chantikul, P., Anstis, G. R., Lawn, B. R. & Marshall, D. B., A critical evaluation of indentation techniques for measuring fracture toughness: II, Strength method. *J. Am. Ceram. Soc.*, **64** (1981) 539–43.
30. Koyama, T., Uchida, S. & Nishiyama, A., Effect of microstructure on mechanical properties and cutting performance of Al_2O_3-Ti(C,N) ceramics. *J. Ceram. Soc. Japan (Int. Edn)*, **100** (1992) 520–4.
31. Krell, A. & Klaffke, D., Effects of grain size and humidity on fretting wear in fine-grained alumina, Al_2O_3/TiC, and zirconia. *J. Am. Ceram. Soc.*, **79** (1996) 1139–46.